International Journal of GEOMATE, Feb., 2025 Vol.28, Issue 126, pp.52-60
ISSN: 2186-2982 (P), 2186-2990 (O), Japan, DOI: https://doi.org/10.21660/2025.126.4764
Geotechnique, Construction Materials and Environment

ANALYSIS OF SEDIMENT CHARACTERISTICS AND FLOW DYNAMICS AFTER NORMALIZATION OF THE CITARUM-MAJALAYA RIVER IN INDONESIA

*Joko Nugroho[1], Martha Natalia Pirsouw[1], Siska Wulandari[1], Indratmo Soekarno[1], Arno Adi Kuntoro[1], Siti Aisyah Nurul Qolbi[1], and Faizal Immaddudin Wira Rohmat[1]

[1]Faculty of Civil and Environmental Engineering, Institut Teknologi Bandung, Indonesia

*Corresponding Author, Received: 16 Oct. 2024, Revised: 09 Dec. 2024, Accepted: 13 Dec. 2024

ABSTRACT: The Citarum-Majalaya River is frequently inundated by annual flooding. The floods carry sediment material and sedimentation up to 25 cm in some locations. Structural efforts to maintain river capacity have been made by normalizing the river in 2021, but significant flooding occurred again in 2023. This study analyzes sediment transport dynamics in the Citarum-Majalaya River. Data collection includes secondary data from previous erosion and sedimentation studies in the watershed. The primary data was obtained by direct measurement in the upstream and downstream under two water level conditions. The findings of data analysis and laboratory testing indicate that the type of flow in the Citarum-Majalaya River section is turbulent and subcritical, and the type of sediment is sand and clay, with distinct sediment movement patterns between upstream and downstream. The turbulent and subcritical flow allows particles to remain suspended for longer periods and settle more rapidly when the flow decreases, predicting high sedimentation levels in this river and reducing the river's capacity.

Keywords: Majalaya, Flood, Sediment transport, Sedimentation, Riverbed morphology changes

1. INTRODUCTION

Floods can cause damage problems and significant loss of life and property damage [1]. In densely populated areas, floods require particular attention due to potentially significant losses [2,3]. The risk of urban flooding is driven by three main elements: physical environment, public awareness and urbanization, and policy and long-term changes [4]. Flooding typically occurs in lowland watershed areas, where rainwater accumulates and channels through streamflow to rivers. When heavy rainfall occurs, the increased streamflow can exceed the river's capacity, causing water overflow and flooding [5,6]. Moreover, river capacity can also be reduced due to sediment accumulation, causing riverbed shallowing, further decreasing the river's water capacity and increasing flood risk [7].

Sediment transport is a vital process in river systems, referring to the process of moving solid particles through the action of gravity and fluid flow, which is crucial for shaping river landscapes and affecting water quality [8]. It consists of two main processes: degradation and aggradation, determined by the balance of shear stress (force by water flow) against critical stress (the resistance of sediment to movement) [9]. Degradation occurs when shear stress overcomes critical stress, dislodging particles to move downstream, known as erosion. Conversely, aggradation occurs when shear stress falls below critical stress, causing particles to settle, which can lead to channel narrowing and increased flood risk, referred to as sedimentation. The accumulation of sediment in rivers can significantly reduce channel discharge capacity and pose a challenge towards increased flood risk in the future [7].

The Majalaya region, located within the Majalaya watershed of Indonesia, is part of the Upper Citarum Watershed (UCW) [10]. This area faces high erosion and sedimentation rates due to land cover changes, rapid population growth, and altered land use [11,12]. Its flat topography makes it prone to frequent flooding [5]. The local community has about six flood events annually, with water levels reaching ankle height in major urban areas and up to one meter near riverbanks [13]. The floods typically rise rapidly within one to two hours after rainfalls [13]. Along with the flood that occurred, this flooding often left sediment deposits so that when the flood retreated, some places reached 25 cm in height on the roads, as observed by the residents. Mitigation efforts have been implemented to address this issue, focusing on engineering constructions designed to reduce flood volumes [14]. The Citarum River Regional Office (Balai Besar Wilayah Sungai Citarum, BBWSC) has completed a river normalization project along a 5.4 km stretch in the Citarum-Majalaya River segment from 2019 to 2021. This project involves infrastructure improvements, such as reinforcing riverbanks, dredging, and removing obstructions to improve river flow and capacity, ultimately aiming to reduce the flood risk.

Despite the normalization in 2021, flooding reoccurred on April 26, 2023, affecting 227.86 hectares, indicating that the sediment dredging in the Citarum-Majalaya river area provided only a

temporary solution. Sediment accumulation (Fig. 2b) significantly reduces the river's capacity to manage water flow, leading to floods. A comprehensive analysis of how sediment contributes to capacity changes is essential in line for accurate flood discharge predictions, as it significantly influences the river's hydrology behavior [15]. Gaining insights into these relationships is vital for effective river system management and mitigating issues related to sediment accumulation.

This study focuses on investigating how sediment transport dynamics contribute to the continuing flooding in normalized river systems on the Citarum-Majalaya River. Understanding these dynamic processes is crucial for predicting river behavior, developing more effective flood mitigation strategies, and improving the resilience of communities in flood-prone regions. Field data collection and laboratory testing were conducted to look at both suspended and bed load concentration, as well as flow rates, at two locations along the river. Our analyses use several formulas, including Einstein, Meyer-Peter and Müller (hereafter MPM) and the Rouse method. The insights gained from these analyses are expected to expound the sediment transport processes within this river. The outcomes of this study may inform future river management strategies and engineering interventions, leading to more sustainable practices in flood control within this river.

2. RESEARCH SIGNIFICANCE

The investigation of sediment characteristics in the Majalaya—a flood-prone area—is crucial for a comprehensive understanding of river morphodynamics and sediment dynamics. By analyzing factors such as concentration, particle size distribution, and total suspended solids, this research serves as preliminary information to assess the potential reduction in hydraulic capacity, which contributes to flooding despite normalization efforts. This examination offers important insights into the mechanisms of sediment transport in riverbed geometry that contribute to channel siltation. This investigation improves understanding of river system dynamics and presents actionable solutions for sustainable river management and community protection against flood-related hazards.

3. MATERIALS AND METHOD

3.1 Research Workflow

Fig. 1 shows the research workflow of the study. The first step is the data collection, including primary and secondary data. The primary data—which is sediment samples and hydraulics data—were collected through field measurements. The sediment samples were then processed through analysis in the laboratory, and the resulting value parameters were analyzed for sediment transport analysis. Table 1 lists the measured field data collected in this study, and the sampling location is shown in Fig. 2a.

The sediment and hydraulics characteristics and riverbed morphology change data were combined and analyzed to evaluate the impact of sediment transport patterns related to riverbed morphology change and flood risk assessment.

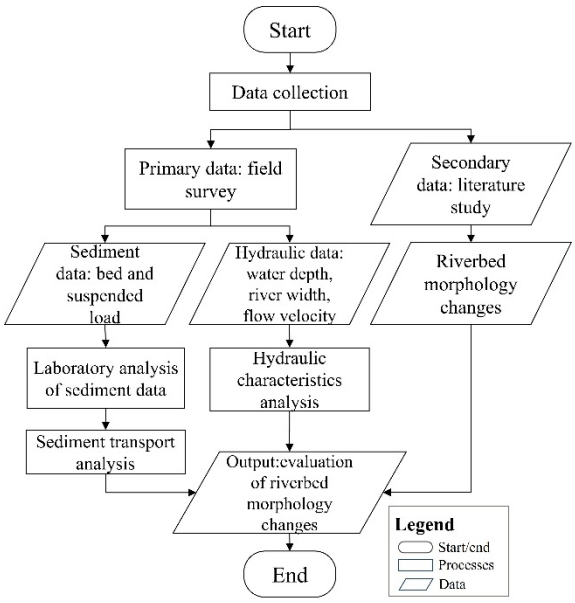

Fig. 1 Research workflow

3.2 Data Collection and Types of Data Used

The data used in this study was taken from the site in the Majalaya River in March 2024 during the low-flow conditions. Table 1 outlines the types of primary data collected and the equipment used for the acquisition. These data are direct sediment measurements gathered directly from the site, and experiments were performed.

Table 2 shows the secondary data collected from literature reviews such as previous studies and historical records published from several sources and related instances upon request.

Table 1. Details of primary data used in this study

Data Type	Tools	Source
Flow Velocity	Current Meter type TH-031	MFD
Bed Load	Grabber sampler	MFD
Suspended load	US-DH 59 sampler	MFD
Transport Rate	Helley-Smith sampler	MFD

Note: MFD = Measured Field Data.

Table 2. Details of secondary data used in this study

Data Type	Tools	Source
Citarum River Profile	Topography Data (Cross-section) in 2009, 2020 and 2022	BBWSC
Previous research	The number of erosion results with USLE to determine the amount of Sediment Yield.	[11]

3.3 Site Selection and Study Area Description

Specifically, the study site is in the Citarum-Majalaya River, Majalaya City, Indonesia. This city is crossed by the Citarum River, the largest and longest river in West Java, one of the strategic rivers in Indonesia [16]. The sediment data for this study were collected from two sampling locations around the Sasak (bridge) along the river. The bridges were chosen because of their accessible to the entire width of the river, allowing for easy and safe sampling across the river width and consistent location of collection of water and sediment samples from various points along the river cross-sections. The upstream location at the Sasak Citarum Majalaya is shown in Fig. 2a at point (A) with a green color. The downstream, at the Sasak Citarum Leuwidulang, is shown in yellow in Fig. 2a at point (B). From each location, three bedload and suspended load sediment samples were collected.

The impact of sediment on river flooding in Majalaya by minimizing the river capacity is analyzed by comparing the maximum changes in riverbed values over different periods [17]. Remarkably, the maximum elevation difference was calculated before normalization (elevation in 2020 minus elevation in 2009) and after normalization (elevation in 2022 minus elevation in 2020). Previous studies have explored the comparison of maximum river bedload in the Majalaya River [18]. Fig. 3b shows the comparison spans 11 years before normalization and two years after normalization in the river cross-section. The results indicate that the changes occurring within 2 years after normalization are higher than the 11 years before normalization, indicating a sediment accumulation and leading to a decrease in the river's storage capacity so that during extreme rainfall conditions, the potential for water overflow becomes faster [18].

3.4 Hydraulic and Sediment Sampling Method

Field data was collected on February 28 and March 1, 2024, using the equipment in Table 1. Measurements were taken at two locations (A and B) under two different water level conditions: 1.40 m and 1.52 m, as recorded by an Automatic Water Level Recorder (AWLR) at the bottom of the Sasak Citarum Majalaya bridge [13]. Three sampling points were established across the river width at each location and water level. The study involved measuring the wet cross-section depth for area calculation, recording flow velocity at 0.6d depth (Fig. 3), and collecting hydraulics data including hydraulics radius (R), wetted perimeter (P) and slope (S_f). These data are required to measure the river flow discharge in open channels, the procedure as in Indonesian National Standards (SNI) 8066:2015. The detailed analysis results are well presented in Table 3.

The sediment sampling process uses a Helley Smith sediment sampler for collecting bedload samples [19]. Suspended load samples were collected using a US-DH-59 depth-integrating sampler as in SNI 3414:2008. Additionally, a Grabber sampler was utilized to obtain bed material. The Helley Smith Sampler was used to determine the bed load transport rate, while the Grabber was used to study sediment characteristics. In this study, the processed bed load samples from the laboratory will undergo review, including sieve analysis and specific gravity testing. Suspended load sampling was carried out with the sampling point adjusted to the flow velocity sampling point and then tested for Total Suspended Solids (TSS).

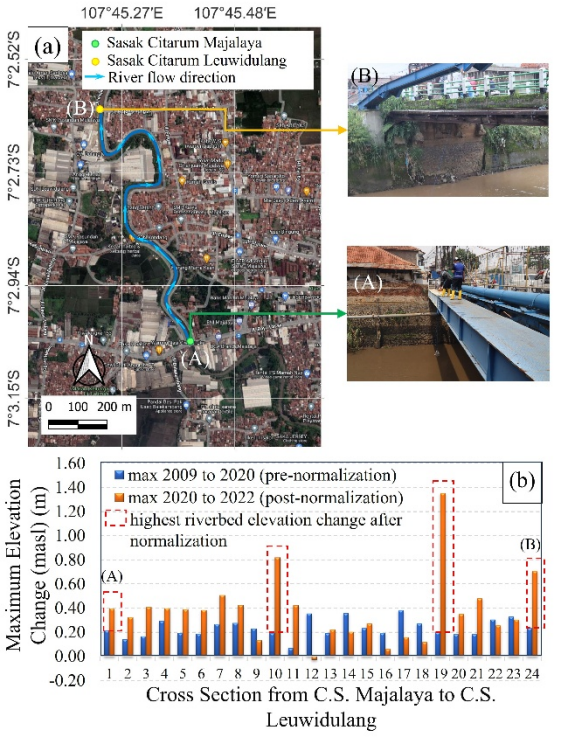

Fig. 2 (a) The location of sediment data collection, (b) Comparison of maximum riverbed changes between locations A-B in 24 sections before and after normalization

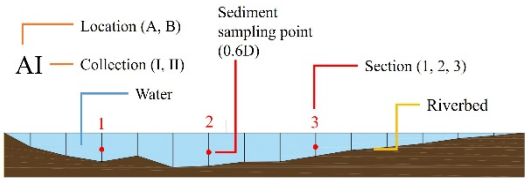

Fig. 3 The illustration of the data collection name. Sampling takes place in two locations (A and B), each with two collections (I and II), and each collection includes three data sections (1,2 and 3)

3.5 Laboratory Data Processing

The laboratory data processing is conducted in two different locations at the Institut Teknologi Bandung (ITB) laboratory. There were a total of 12 (twelve) samples tested and labeled as locations, collections, and sections (AI1, AI2, AI3, BI1, BI2, BI3, AII1, AII2, AII3, BII1, BII2, and BII3).

Grain size (sieving) and specific gravity tests were conducted at the Soil Mechanics Laboratory at ITB Ganesha campus with American Society for Testing and Materials (ASTM) standards. The grain size processes were documented in the Fig. 4, while the specific gravity test was documented in the Fig. 5.

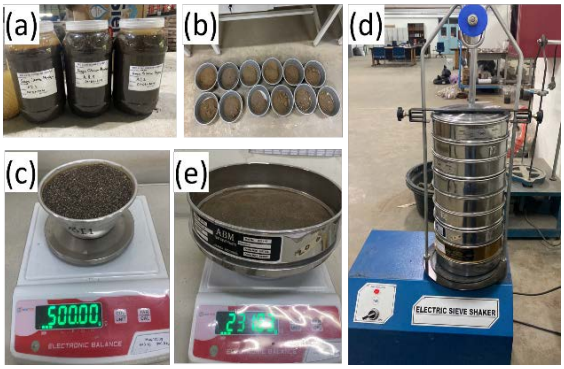

Fig. 4 Documentation of the sieve analysis test includes the following steps: (a) preparing samples collected from the field; (b) drying the sample until the water content is removed (with three weighing to ensure consistent weight); (c) weighing the total amount of samples for analyzed by sieve; (d) sieving process with a sieve shaker using sieves set in the order from top #4, #10, #20, #40, #40, #60, #100, #200, #400 sieve, and pan for 15 minutes; and (e) weighing the weight of the sample retained on each sieve after sieving. The cumulative retained percentage (percent finer) is depicted in the Fig. 9.

The TSS test was conducted at the Laboratory of Environmental Infrastructure Engineering at ITB Jatinangor campus. The testing was performed as per guidelines in SNI 06-6989.3-2004. The laboratory testing processes are documented in Fig. 6. The results are applied to a diverse range of empirical and theoretical formulas, with parameters provided in this study, allowing for the identification of suitable criteria for sediment characteristics.

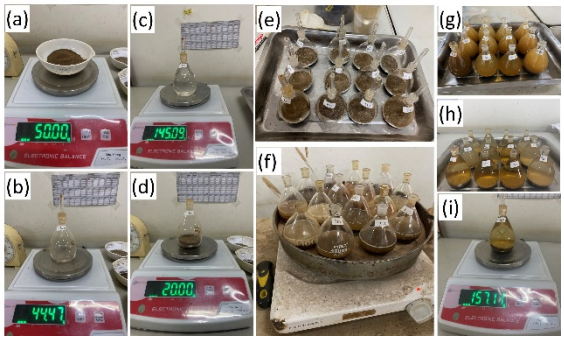

Fig. 5 Documentation of specific gravity test includes the following steps: (a) weighing the soil samples passing through a No. 10 sieve; (b) weighting the empty pycnometer; (c) weighting the pycnometer filled with distilled water; (d) weighting the pycnometers containing the soils; (e) preparing all samples to be filled with distilled water; (f) heating the pycnometers containing the soils and water until boiling and trapped air bubbles are removed (g) refilling the pycnometers with distilled water to the top after the boiling process; (h) allowing the boiled samples to rest undisturbed for 24 hours to ensure thermal equilibrium and complete saturation; and (i) weighting the pycnometer containing the soil and distilled water after 24-hour resting period.

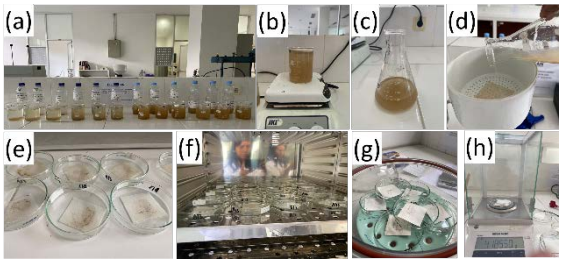

Fig. 6 TSS testing documentation: (a) 12 samples were transferred to a glass beaker; (b) the test sample was homogenized using a magnetic stirrer on a hot plate; (c) using a pipette, the sample was homogenized up to a volume of 100 ml; (d) the sample was then placed on a filter paper previously rinsed with distilled water; (e) the filter paper was lifted and placed on a beaker containing the coded sample; (f) all Petri dishes and filter paper were placed in an oven at 105°C for one hour; (g) all samples were cooled in a desiccator for 15 minutes; (h) Petri dishes and filter paper were weighed using analytical balances to obtain the resulting weight.

3.6 Sediment Analysis

The sediment transport approach utilizes several equations developed or utilized by previous

researchers. The selection is quite challenging due to the characteristics of sediment research, which is a unique site. Rivers have different hydraulic and morphological characteristics such as discharge, velocity, energy slope, bedforms, median diameter, and sinuosity [26]. This study uses the Einstein (1950) [21] and Meyer-Peter Müeller (MPM) (1948) [22] formulas for bed load estimation. These equations contain the least amount of inaccuracy compared to other equations, according to validation by Ali et al. [26]. For suspended load estimation, the Rouse (1937) formula [23] is utilized.

a. Einstein (1950) [21]

$$q_b = \phi\sqrt{g\Delta {D_{50}}^3} \quad (1)$$

Where q_b is bedload transport rate ($m^3/s/m$); Φ is the sediment transport intensity (dimensionless)($\phi = 40(1/\psi)^3$); g is the gravitational acceleration (9,81 (m/s^2)); Δ is the relative submerged density of sediment particles ($\Delta = s - 1$) with s the specific density of the sediment grains; D_{50} is the particle diameters of bed materials; ψ is the bed shear stress/mobility parameters (Einstein parameters); $\psi = (\Delta D_{50})/(\mu RS) = 1/{F_{rd}}^2$; μ is the ripple factor ($\mu = 1$); R is the hydraulic radius; S is the energy slope; d is the flow depth (m); F_{rd} is the Froude number.

b. Meyer Peter Muller (1948) [22]

$$q_b = 8\sqrt{\Delta g {D_{50}}^3}\left[\left(\frac{\mu RS}{\Delta d} - 0.047\right)\right]^{3/2} \quad (2)$$

Where $\mu = \left(C_{channel}/C_{grain}\right)^{3/2}$, C is the Chezy's coefficient given by $C_{chanel} = v/\sqrt{RS}$ and $C_{grain} = 18\ log(12R/D_{90})$. D_{50} and D_{90} is the particle diameters; 0.047 is the critical Shields value for initiation of particle motion.

c. Rouse (1937) [23]

$$\frac{C}{C_a} = \left(\frac{D-y}{y}\frac{a}{D-a}\right)^{Ro} \quad (3)$$

Where C and C_a are the concentration of sediment having fall velocity w at vertical distances y and an above the bed and D= total depth; Ro is the Rouse parameter where $Ro = w_s/(ku_*)$. k is the von Karman's constant (0.4); u_* is the shear velocity where $u_* = \sqrt{ghS_o}$. w_s is the settling velocity where $w_s = \frac{1}{18}\frac{\gamma_s - \gamma}{\gamma} g \frac{{d_s}^2}{v}$; d_s is the representative diameter of the suspended sediment particles; γ_s and γ are the specific weights of the sediment and water; v is the kinematic velocity; h is the flow depth and S_o is the channel bed slope (dimensionless).

4. RESULT AND DISCUSSION

4.1 Sediment Delivery Ratio and Sediment Yield Estimations in The Majalaya Watershed

The amount of sediment carried by the natural stream is much less than the total erosion occurring in the upstream watershed [24]. Sediment is deposited along the source to the stream whenever the water flow is not strong enough to transport it. The watershed Sediment Delivery Ratio (SDR) is the ratio of sediment reaching the outlet to the total sediment load generated by the watershed [25].

The sediment yield (Y) is calculated using the formulas by Boyce by $Y = A_t SDR$, where Y is the sediment yield, A_t is the drainage area of the upstream watershed, and SDR is the sediment delivery ratio calculated by $\mathrm{SDR} = 0.41\mathrm{A_t}^{-0.3}$. The SDR is influenced primarily by the upstream watershed's drainage area, A_t. It decreases as the increase in area due to the possibility of sediment trapped in upland areas by lakes, reservoirs, and flood plains.

Research by Kardhana et al. [11], indicates that the erosion rate of the Majalaya watershed is considered moderate at 173 tons/ha/year with a catchment area of 205.45 km^2. This results in an SDR of 0.0829, estimated that only 8% of the total eroded sediment in the watershed reaches the outlet, while 92% is retained, deposited, or settled before reaching the outlet, possibly due to vegetation, topography, or sediment control structure. The estimated sediment yield is 17.03 tons/km^2/year, suggesting that about 17.03 tons of sediment are transported anually from the watershed into the river. This number could rise if changes in land use, particularly if bare land increases and forested areas decrease, exacerbating erosion and sedimentation issues in the watershed [10].

4.2 Hydraulic Characteristics of The Citarum-Majalaya River

Flow velocity data collection is performed concurrently with measuring the width and depth of the wetted cross-section to determine the river's cross-sectional area. The river flow can be calculated for each sampling location using these numbers. Additionally, several key sectional parameters can be derived from the field measurements presented in Table 3. Manning's value is based on surface roughness and Manning's 'n' in Chow's table (1959). The analysis indicates that the value of the Froude number is less than 1 for each cross-section, indicating subcritical flow. Additionally, the Reynold number in the open channel exceeds 12,500, signifying the turbulent flow [26].

Table 3. Summary of hydraulic characteristics analysis by cross-section

Sampling Code	A	v	Q	d	l	P	R	n	S_f	τ_b	Re	Fr
AI	10.15	1.02	10.35	0.98	13.85	17.40	0.58	0.025	0.001	7.60	593,329	0.328
BI	9.14	0.94	8.48	0.92	14.91	18.22	0.50	0.025	0.001	6.83	472,293	0.314
AII	13.40	1.16	14.98	1.23	13.85	18.30	0.73	0.025	0.001	9.09	846,442	0.332
BII	10.88	1.02	10.61	1.06	14.91	18.74	0.58	0.025	0.001	7.66	592,342	0.316

Note: A is the Cross-sectional area (m^2), v is the flow velocity (m/s), Q is the calculated river flow (m^3/s), d is the cross-sectional depth (m), l is the cross-sectional width (m), P is the wetted perimeter (m), R is the hydraulic radius, n is the manning, S_f is the frictional slope, τ_b is the shear stress, Re is the Reynold number, and Fr is the Froude number. R, n, S_f, τ_b, Re, and Fr is a dimensionless number.

4.3 Laboratory Sediment Test Result and Sediment Parameters

4.3.1 Suspended load analysis

Fig. 7a shows the total suspended load of each cross-section. At location A (upstream), the suspended sediment concentration (Cs) at AII is lower than at AI. The increases in water flow decrease the Cs value. On the other hand, the downstream (location B), the Cs value is higher at the increase of river flow, as is the second collection (BII). The difference in Cs value can be attributed to the Reynolds number (Re) (Table 3). Reynold number is a dimension number that affects turbulent flows in open channels. In terms of location, location A has a higher Re than in location B, consistent across both collection events. The upstream area (AI) exhibits a higher Cs when the flow is smaller in Collection I, while the downstream (BI) has a greater Cs at the higher flow. Turbulent flow with high Re tends to transport sediment efficiently, especially suspended sediment, allowing it to retain the sediment in suspension longer, thereby increasing the concentration, especially in subcritical flow, making the sediment can't transport far [27]. This result indicates that changes in flow characteristics, especially turbulence, significantly affect suspended sediment behavior and distribution.

The suspended sediment load (Qs) is computed as the product of suspended sediment concentration (Cs) and river flow (Q). Fig. 7b illustrates the suspended sediment load for each location and collection, which correlates directly with sediment concentration in each location and collection. The results suggest that the suspended sediment load (discharge) (Qs) is primarily influenced by two factors: 1. Sediment concentration: Higher concentrations of dispersed sediment particles in the water flow lead to an increase in suspended sediment load (Qs), 2. River flow characteristics (Q): Larger Q values provide greater water volume for sediment transport, enhancing Qs. The river flow is affected by flow velocity (v): faster v increases the water's capacity to lift and carry suspended sediment.

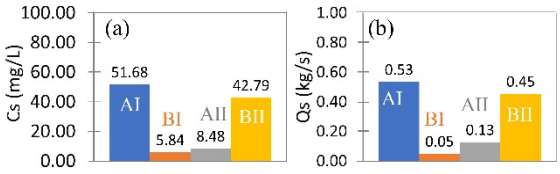

Fig. 7 (a) Average suspended sediment concentration (Cs) and (b) the suspended sediment load (Qs) per cross-section

The Rouse method (eq. 3) calculates the vertical distribution of sediment concentration at a specific height in the water column [28]. The variable C_a represents the reference sediment concentration at a reference elevation "a" above the bed elevation. The relative concentration C/Ca depends on the elevation y above the reference elevation as derived by Rouse [23]. Fig. 8 describes the interval of the sediment concentration distributed at each collection point.

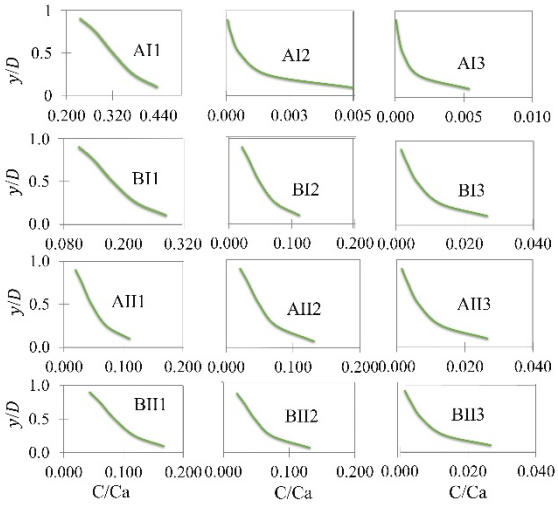

Fig. 8 Suspended sediment concentration profiles using the Rouse method

From the calculation, the magnitude of the sediment concentration profile value varies greatly. The sediment concentration profile values vary due to the variance in slope at each collection point, which

impacts the friction velocity (u^*) and the settling velocity (ωs) of the bed load sediment particles. Based on the result, it can be concluded that curves decreasing as y/D increase indicate that higher sediment concentrations are found closer to the bed, while lower concentrations are closer to the water surface.

4.3.2 Bed load analysis

The critical particle size for distinguishing various transport mechanisms varied among different types of soils. This indicates that sediment transport behavior is not uniform and is influenced by specific soil characteristics, such as the content of clay and sand. The size of sediment particles, including clay and sand, affects how they are transported by water. The bedload samples were collected at each sampling point using a Grabber sampler to determine the characteristics of the soil. The result of the Sieve analysis from the test samples in Fig. 4 are classified by class according to Wentworth (1922) [29] and presented in Fig. 9. Based on the particle size, the sediments at the study location can generally be classified into three classes: granules (gravel), sand, and silt.

On average, the characteristics of bed load sediment in location A are quite different from those in location B. Location A has the percentage of sand and clay as 52% and 48%, respectively. In location B, the percentages are 37% and 63%, respectively. The higher percentage of sand in the upstream (A) indicates that the sedimentation rate in the upstream is higher than in the downstream (B). While larger particles like sand tend to settle more quickly, smaller and finer particles like clay require a longer settling time [30]. A comparison of empirical methods, MPM and Einstein, with field data using Helley Smith (Fig. 10) indicates that both method do not fully captures real conditions. However, MPM is closer to accuracy as it yields smaller values.

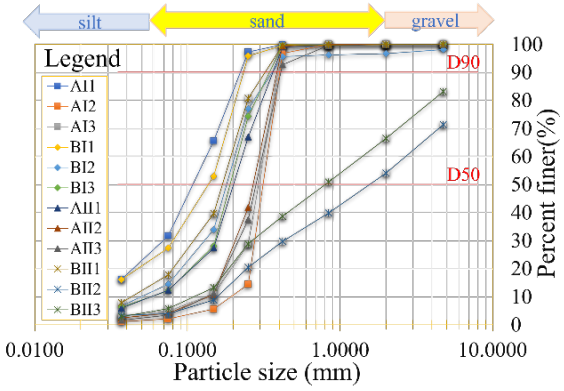

Fig. 9 Sieve analysis results from 12 samples collected in the site location with median grain sizes D50 and D90

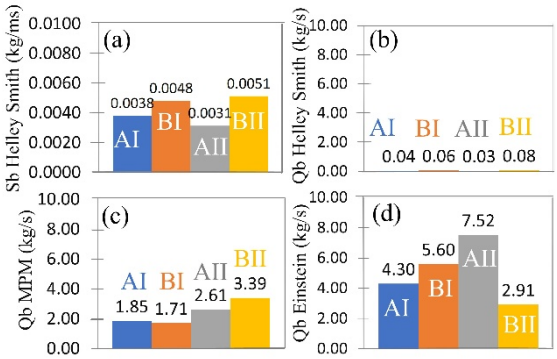

Fig. 10 (a) Bed Load transport rate from the Helley Smith sampler. Total bed load rate per cross-section from the (b) Helley Smith calculation, (c) MPM, and (d) Einstein Method

4.4 Impact of Sediment Characteristics on Riverbed Morphology and Flood Risk Assessment

Sediment transport in rivers is primarily affected by sediment size, flow velocity, and riverbed roughness. The movement of these particles is influenced by hydrodynamic drag and lift, which vary with the flow velocity and gradient near the riverbed [31]. The sediment discharge ratio significantly depends on the water depth in rivers with fine materials. Despite appearing delicate, the sediment in the Citarum-Majalaya River from laboratory sieve analyses is classified as sand, highlighting the importance of sediment type in transport dynamics. Analysis of sediment rate and concentration across various locations, flow conditions, and sections reveals diverse sediment movement patterns, indicating that morphological changes are significantly influenced by flow velocity and sediment transport, shaping distinct river sections.

The profile of suspended sediment concentration distribution by the Rouse method showed different values at each sampling point and depth. This variability was due to differences in cross-sectional heights at the measurement points and varying slopes, affecting the friction velocity and sedimentation/fall velocity. As a result, the distribution area of the suspended sediment concentration profile was not uniform.

When the depth exceeds 1 meter, the depth-integrating sampler can measure over 80% of the total sediment load. Analysis of the bed load showed significant variations in sediment levels within different cross-sections due to river flow and grain size. Testing TSS concentrations revealed different results under two water level conditions. For accurate sediment analysis during floods, it is important to measure data, flow velocity and sediment transport, including suspended and bed loads, under flood or peak flow conditions [32]. Since this area is part of the Bandung basin, monitoring and paying attention to sediment transport along the Citarum River in this

region is crucial. The monitoring results will provide valuable insights for the following research in this area.

5. CONCLUSION

This study analyzed sediment characteristics and river flow dynamics in the flood-prone Majalaya City, Indonesia, focusing on the Citarum-Majalaya River. Data collection occurred at two locations: upstream Sasak Citarum Majalaya (A) and downstream Sasak Citarum Leuwiulang (B), at two water levels of 1.40 m and 1.52 m. 12 data points were collected across three sections per location and water level. The result revealed that hydraulic conditions and sediment grain properties significantly influenced post-normalization sediment transport dynamics, resulting in distinct sediment movement patterns between upstream and downstream areas. The subcritical and turbulent flow influences the concentration and makes retained sediment likely to settle, contributing to sedimentation, elevating the riverbed, and reducing channel capacity. The results of this study can be used for further research in the form of 2D-sediment transport modeling to obtain a more in-depth analysis of locations that have the potential for erosion and sedimentation along the river channel.

6. ACKNOWLEDGMENTS

This research is partially supported by PPMI FTSL ITB.

7. REFERENCES

1. Sulong, S.; Romali, N.S., Flood Damage Assessment: A Review of Multivariate Flood Damage Models, International Journal of GEOMATE, Vol.22, Issue 93, 2022, pp. 106–113.
2. Cea, L.; Costabile, P., Flood Risk in Urban Areas: Modelling, Management and Adaptation to Climate Change: A Review, Hydrology, Vol. 9, Issue 3, 2022, pp. 20-54.
3. Enung; Kusuma, M.S.B.; Kardhana, H.; Suryadi, Y.; Rohmat, F.I.W. Hourly Discharge Prediction Using Long Short-Term Memory Recurrent Neural Network (LSTM-RNN) in the Upper Citarum River. International Journal of GEOMATE, Vol. 23, Issue 98, 2022, pp. 147–154.
4. Berndtsson, R.; Becker, P.; Persson, A.; Aspegren, H.; Haghighatafshar, S.; Jönsson, K.; Larsson, R.; Mobini, S.; Mottaghi, M.; Nilsson, J.; et al., Drivers of Changing Urban Flood Risk: A Framework for Action, J. of Environmental Management, Vol. 240, 2019, pp. 47–56.
5. Rohmat, F.I.W.; Sa'adi, Z.; Stamataki, I.; Kuntoro, A.A.; Farid, M.; Suwarman, R., Flood Modeling and Baseline Study in Urban and High Population Environment: A Case Study of Majalaya, Indonesia, Urban Climate, Vol. 46 2022, p. 101332.
6. Burnama, N.S.; Rohmat, F.I.W.; Farid, M.; Kuntoro, A.A.; Kardhana, H.; Rohmat, F.I.W.; Wijayasari, W., The Utilization of Satellite Data and Machine Learning for Predicting the Inundation Height in the Majalaya Watershed, Water (Switzerland), Volume 15, Issue 17, 2023, p. 3026.
7. Hauer, C.; Wagner, B.; Aigner, J.; Holzapfel, P.; Flödl, P.; Liedermann, M.; Tritthart, M.; Sindelar, C.; Pulg, U.; Klösch, M.; et al., State of the Art, Shortcomings and Future Challenges for a Sustainable Sediment Management in Hydropower: A Review, Renewable and Sustainable Energy Reviews, Volume 98, 2018, pp. 40–55.
8. Dasgupta, P., Sediment Gravity Flow—the Conceptual Problems, Earth-Science Reviews, Vol. 62, Issues 3-4, 2003, pp. 265–281.
9. Maini, M.; Kironoto, B.A.; Rahardjo, A.P.; Istiarto, I., Flow Characteristics of Equilibrium and Non-Equilibrium Sediment Transport Flows, International Journal of GEOMATE, Vol. 25, Issues 110, 2023, pp. 77–86.
10. Rixson, L.; Wenbiao, D.; Aliyanta, B.; Godbold, D.; Lubis, A.A.; Nugraha, E.D. Assessment of Soil Erosion in the Upper Citarum Watershed for Sustainability of the Saguling Reservoir: Unmixing Model Approach, Environmental Monitoring and Assessment, Vol. 196, Issues 7, 2024, p. 615.
11. Kardhana, H.; Solehudin; Wijayasari, W.; Rohmat, F.I.W., Assessing Basin-Wide Soil Erosion in the Citarum Watershed Using USLE Method, Results in Engineering, Vol. 22, 2024, p. 102130.
12. Chaidar, A.N.; Soekarno, I.; Wiyono, A.; Nugroho, J., Spatial Analysis of Erosion and Land Criticality of the Upstream Citarum Watershed, International Journal of GEOMATE, Vol. 13, Issue 37, 2017, pp. 133–140.
13. Dewa Gede A Junnaedhi, I.; Riawan, E.; Suwarman, R.; Wahyu Hadi, T.; Lubis, A.; Joko Trilaksono, N.; Rahayu, R.; Kombara, P.; Waskito, R.; Ekalaya Oktora, H.; et al., Majalaya Flood Early Warning System: A Community Based Approach, Conference proceedings, in Proc. IOP Conf. Ser.: Earth Environ. Sci., 2017, Vol. 71, p. 012013.
14. Yang, T.H.; Liu, W.C., A General Overview of the Risk-Reduction Strategies for Floods and Droughts, Sustainability (Switzerland), Vol.12, Issue 7, 2020, p. 2687.
15. Pranatan, A.Y.; Soekarno, I.; Moerwanto, A.S.; Nugroho, E.O.; Manurung, E.J.P.; Sari, I.K.,

River Capacity Prediction Based on Flood Discharge Probability Scenario and Sediment Transport Consideration: Study Case in Sayung River, Conference proceedings, in Proc. IOP Conf. Ser.: Earth Environ. Sci., 2024, 1290, p. 012040.
16. Rohmat, F.I.W.; Stamataki, I.; Sa'adi, Z.; Fitriani, D., Flood Analysis Using HEC-RAS: The Case Study of Majalaya, Indonesia under the CMIP6 Projection, EGU General Assembly 2022, 2022, p. EGU22-3090.
17. Gunawan, T.A.; Kusuma, M.S.B.; Cahyono, M.; Nugroho, J., The Application of Backpropagation Neural Network Method to Estimate the Sediment Loads, Conference proceedings, in Proc. Sriwijaya Int. Conf. on Engineering, Science and Technology (SICEST 2016) on MATEC Web Conf., Vol. 101, 2017, p. 05016.
18. Pirsouw, M.N.; Nugroho, J.; Wira Rohmat, F.I.; Burnama, N.S.; Kuntoro, A.A.; Farid, M.; Kardhana, H., Study of Sediment Transport Distribution Pattern after Normalization in the Majalaya Area, Citarum River, In Proc. 9th Int. Conf. on Climate Change on E3S Web of Conf., Vol. 467, 2023, p. 01028.
19. Gaudet, J.M.; Roy, A.G.; Best, J.L., Effect of Orientation and Size of Helley-Smith Sampler on Its Efficiency, Journal of Hydraulic Engineering, Vol. 120, Issue 6, 1994, pp. 758-766.
20. Ali, H.L.; Mohammed, A.; Yusuf, B.; Aziz, A.A., Testing The Accuracy of Sediment Transport Equations Using Field Data, Malaysian J. of Civil Engineering, Vol. 28, Issue 1, 2016, pp. 50-64.
21. Einstein, H.A., The Bed-Load Function for Sediment Transportation in Open Channel Flows, A Report in Tech. Bull. No. 1026, U.S. Department of Agriculture: Washington, DC, USA, 1950, pp. 1-89.
22. Meyer-Peter, E.; M.R., Formulas for Bed-Load Transport., in Proceedings of the 2nd Meeting of the Int. Association for Hydraulic Structures Research, Delft: The Netherlands, 1948, pp. 39-64.
23. Rouse, H., Modern Conceptions of the Mechanics of Fluid Turbulence, Transactions of the American Society of Civil Engineers, Vol. 102, 1937, pp. 463–505.
24. Julien, P.Y., Erosion and Sedimentation; 2nd ed., A Book Cambridge University Press: New York, 2010, pp. 1-390.
25. Woznicki, S.A.; Nejadhashemi, A.P., Spatial and Temporal Variabilities of Sediment Delivery Ratio, Water Resources Management, Vol. 27, 2013, pp. 2483–2499.
26. Bengtson, H.H., CE-089 Manning Equation for Open Channels, COURSE CONTENT, PDH Star, pp. 1-42.
27. Kumar, P.; Sharma, A., Reynolds Number Effect on the Parameters of Turbulent Flows over Open Channels, AQUA - Water Infrastructure, Ecosystems and Society, Vol. 73, Issue 5, 2024, pp. 1030–1047.
28. Eggenhuisen, J.T.; Tilston, M.C.; de Leeuw, J.; Pohl, F.; Cartigny, M.J.B., Turbulent Diffusion Modelling of Sediment in Turbidity Currents: An Experimental Validation of the Rouse Approach, The Depositional Record, Vol. 6, Issue 1, 2019, pp. 203–216.
29. Wentworth, C.K., A Scale of Grade and Class Terms for Clastic Sediments, The J. of Geology, Vol. 30, Issue 5, 1922, pp. 377–392.
30. Liu, Y.; Liu, G.; Xiao, H.; Xia, X.; Zhang, Q.; Zhou, Z.; Li, H.; Zheng, F.; Guo, Z.; Liu, D., Sediment Sorting and Transport Mechanism Controlled by Both Soil Properties and Hydraulic Parameters on Hillslopes, J. of Hydrology, Vol. 634, 2024, p. 131069.
31. Alhusban, Z.; Valyrakis, M., Assessing Sediment Transport Dynamics from Energy Perspective by Using the Instrumented Particle, Int. J. of Sediment Research, Vol. 37, Issue 6, 2022, pp. 833–846.
32. Jiken, Y.; Watanabe, K.; Saito, N., Study on Sediment Grain-Size Measurement and Calculations at Multiple Points on The Sandbar in Class B River, International Journal of GEOMATE, Vol. 25, Issue 104, 2023, pp. 93–100.